

LAMINAR MIXING FLOW IN A STIRRED VESSEL

NADANIELA EGIDI, LUCIANO MISICI
AND RICCARDO PIERGALLINI

*Dipartimento di Matematica e Fisica,
Università di Camerino,
Madonna delle Carceri, I-62032 Camerino, Italy
egidi@camserv.unicam.it*

(Received 17 November 2000; revised manuscript received 4 December 2000)

Abstract: Using finite element method we study the transient motion of fluid particles in a 3D cavity, when the fluid is incompressible viscous and with uniform density. The fluid is mixed under the action of four-blades turbine that is simulated by a velocity function. The mixing quality of the fluid is studied qualitatively, by visualization, and quantitatively, by measuring the indices of diffusion and dispersion.

Keywords: mixing flow, viscous liquids, finite elements

1. Introduction

In this work we consider the mixing of a fluid in a stirred vessel and use computational fluid dynamics to predict the flow field development. The modern approach to the study of mixing in laminar fluid flow applies concepts of the Lagrangian description of the fluid flow. The Lagrangian description uses coordinates that move with particle, where for fluid particle we mean an element of the fluid of negligible size. We consider the case of incompressible viscous (Newtonian) fluid of uniform density and suppose that the fluid is laminar even in the vicinity of the rotating impeller. The numerical simulation is comprised of two phases, computation of the flow field followed by calculation of particle trajectories to analyze the mixing process. To model the flow we use a rotating fluid boundary at the impeller. In order to reproduce that moving boundary we utilize a function that simulates the flow field in the region of the impeller. The mixing is studied utilizing the trajectories of many particles of the fluid to visualize their distribution inside the domain and to construct diffusion and dispersion indices.

2. Mathematical formulation

The governing equations for our fluid in a region $\Omega \times [0, T] \subset \mathbb{R}^3 \times \mathbb{R}$ are described by the incompressible Navier-Stokes equations ([1]):

$$\operatorname{div} \mathbf{u} = 0, \quad (1)$$

$$\frac{\partial \mathbf{u}}{\partial t} - \frac{1}{Re} \Delta \mathbf{u} + (\mathbf{u} \cdot \nabla) \mathbf{u} + \nabla p = \mathbf{f}, \quad (2)$$

$\forall t \in [0, T]$ and $\forall \mathbf{x} = (x_1, x_2, x_3) \in \Omega$, where $\mathbf{u}(\mathbf{x}, t) = (u_1, u_2, u_3)$. If μ is the viscosity of the fluid and ρ is the density of the fluid, ρ and μ are assumed to be uniform and define the key dimensionless flow parameter known as the Reynolds number

$$Re = \frac{\rho L U}{\mu},$$

where U is a characteristic speed and L is a characteristic length.

In this dimensionless formulation the velocity field of the fluid is $\mathbf{u}U$ the position is $\mathbf{x}L$, the pressure of the fluid is $p\rho U^2$ and the body force per unit of mass is $\frac{\mathbf{f}U^2}{L}$.

In particular, the incompressibility condition, $\text{div } \mathbf{u} = 0$, means that the volume occupied by a given set of particles is constant in time.

Scaling the fundamental variables with respect to typical values and constructing dimensionless parameters provides a measure of the relative importance of the various terms in the equations and identifies the dominant physical phenomena, in particular for a large Reynolds number the convective term dominates the viscous one.

To define the problem completely, it is necessary to set appropriate boundary conditions on each part of the boundary of the computational domain and to give initial conditions, prescribing an initial velocity field at $t = 0$. Obviously, this field must satisfy the continuity equation (1). One can prove that in the case of incompressible flow no boundary conditions for the pressure are necessary, emphasizing the fact that the pressure plays a special role in the solution process of the Navier-Stokes equations ([2]).

In this paper we consider only Dirichlet boundary conditions:

$$\mathbf{u}(\mathbf{x}, t) = \mathbf{g}(\mathbf{x}, t) \quad \forall t, \forall \mathbf{x} \in \partial\Omega,$$

where \mathbf{g} must satisfy

$$\int_{\partial\Omega} \mathbf{g} \cdot \mathbf{n} \, dS = 0. \quad (3)$$

Using the finite element method (FEM), we transform the continuous problem into a discrete problem described by a system of non-linear algebraic equations. We consider the Navier-Stokes equations (1) and (2) in the region $\Omega \times [0, T]$ ($\Omega \subset \mathbb{R}^3$) where:

$$\begin{aligned} \Omega &= T_C \setminus C \\ T_C &= \left\{ (x_1, x_2, x_3) \in \mathbb{R}^3 : 0 < x_3 < z_s, x_1^2 + x_2^2 < \left(\frac{r_s - r_i}{z_s} x_3 + r_i \right)^2 \right\} \\ C &= \left\{ (x_1, x_2, x_3) \in \mathbb{R}^3 : z_m \leq x_3 \leq z_M, x_1^2 + x_2^2 \leq (r_C)^2 \right\}. \end{aligned}$$

T_C is a frustrum of right circular cone, with r_i , r_s and z_s the radius of its bottom base, the radius of its top base and its height, respectively. C is a right circular cylinder of radius r_C and height $z_M - z_m$. The relations between them are: $r_i > 0$, $r_s > 0$, $z_s > z_M > z_m > 0$, $\frac{r_s - r_i}{z_s} z_m + r_i > r_C > 0$.

So the boundary of Ω is $\partial\Omega = \Gamma_i \cup \Gamma_0 = \Gamma$, where:

$$\Gamma_i = \partial C, \quad \Gamma_0 = \partial T_C.$$

For the boundary conditions, we consider Γ_0 like a fixed wall, so along Γ_0 velocity must be zero (no-slip condition):

$$\mathbf{u}(\mathbf{x}, t) = \mathbf{0} \quad \forall \mathbf{x} \in \Gamma_0, \forall t.$$

Instead, to model the impeller, we prescribe the speed of the fluid, under the action of a pitched blade turbine with four blades, at the boundary Γ_i of the cylinder C , so

$$\mathbf{u}(\mathbf{x}, t) = \mathbf{g} \quad \forall \mathbf{x} \in \Gamma_i, \forall t.$$

As the velocity function \mathbf{g} must satisfy (3), in the next paragraph we define the function \mathbf{g} in C with the property $\text{div } \mathbf{g} = 0$.

The initial conditions can be given prescribing an initial velocity field at $t = 0$. In particular, we have:

$$\mathbf{u}(\mathbf{x}, 0) = \mathbf{0} \quad \forall \mathbf{x} \in \Omega,$$

because at $t = 0$ the fluid and the impeller are steady.

3. Flow pattern around the impeller (rotating) blades

In cylindrical coordinates, the function \mathbf{g} , giving the fluid speed in the region C under the turbine action, has the form:

$$\mathbf{V}(\rho, \theta, z) = (-\rho \sin(\theta)V_\rho + \cos(\theta)V_\theta, \rho \cos(\theta)V_\rho + \sin(\theta)V_\theta, V_z),$$

where

$$\begin{cases} V_\rho(\rho, \theta, z) = f(\theta) \\ V_\theta(\rho, \theta, z) = \frac{k-1}{2} f'(\theta) \rho + g(\theta) \phi(\rho) \\ V_z(\rho, \theta, z) = -kz f'(\theta) - zg(\theta) \left[\phi'(\rho) + \frac{\phi(\rho)}{\rho} \right] + h(\theta) \varphi(\rho). \end{cases}$$

We have the sum of three pieces f , $g\phi$, $h\varphi$ that have null divergence. In this way, each function \mathbf{V} of this type has the property $\text{div } \mathbf{V} = 0$.

To define the boundary conditions we must introduce the following periodic function:

$$l(l_1, l_0, A, a) = \begin{cases} l_1 + \frac{l_0 - l_1}{2} \left(\cos\left(\frac{2\pi a}{A}\right) + 1 \right) & \text{if } \cos(a) \geq \cos\left(\frac{A}{2}\right) \\ l_1 & \text{if } \cos(a) < \cos\left(\frac{A}{2}\right). \end{cases}$$

We observe that for $a = 0$, $l = l_0$.

In our simulation, we have four impeller blades. At $t = 0$, each blade is located around the segment given by $\theta_i = \frac{i\pi}{2}$, $i = 0, \dots, 3$, $z_0 = \frac{z_m + z_M}{2}$, $r \leq l_b$ (in cylindrical coordinates), where l_b is the length of each blade. They rotate with angular speed $\omega_b = 8\pi$, so at time t they are in $\theta_i(t) = \theta_i + \omega_b t$.

For $t \geq 0.5$, the dragging radial speed of the fluid is $\omega_f l_b$ where $\omega_f = 2\pi$ moreover the fluid near a blade has a further radial speed which is inversely proportional to its distance to the blade and to its radial position, the maximum of this last radial speed is equal to $(\omega_b - \omega_f) l_b = 6\pi l_b$.

As the blades are initially steady we introduce a grading factor

$$s(t) = \begin{cases} \frac{1 - \cos(2\pi t)}{2} & \text{if } t \leq 0.5 \\ 1 & \text{if } t > 0.5, \end{cases}$$

in this way the maximum radial speed, given to the fluid, passes from 0 to $8\pi l_b$ in the time interval $[0, 0.5]$.

In the first example, the blade turbine gives only a radial impulse to the fluid. In particular, under these hypotheses the fluid speed at time t in a point $p \in C$ with cylindrical

coordinates $p = (\rho, \theta, z)$, is defined by $\mathbf{g}(\rho, \theta, z) = \mathbf{V}(\rho, \theta, z - z_0)$ where:

$$\begin{cases} f(\theta) = s(t) \left(\omega_f + \sum_{i=0}^3 f_i(\theta, t) \right) \\ g(\theta) = 0 \\ h(\theta) = 0 \\ \phi(\rho) = 1 \\ \varphi(\rho) = 1 \\ k = 1 \end{cases} \quad (4)$$

$$f_i(\theta, t) = l(0, \omega_b - \omega_f, \frac{\pi}{4}, \theta - \theta_i(t)),$$

in this case $A = \frac{\pi}{4}$.

For example:

$$f_i(\theta, t) = \begin{cases} 6\pi \frac{\cos(8(\theta - \theta_i(t))) + 1}{2} & \text{if } \cos(\theta - \theta_i(t)) \geq \cos(\frac{\pi}{8}) \\ 0 & \text{if } \cos(\theta - \theta_i(t)) < \cos(\frac{\pi}{8}). \end{cases}$$

In the other examples, the blade turbine gives also a vertical impulse to the fluid. So we have $f(\theta)$, $g(\theta)$, $\phi(\rho)$, k , as in (4), while:

$$\begin{aligned} h(\theta) &= s(t) \left(\sum_{i=0}^3 h_i(\theta, t) \right), \\ h_i(\theta, t) &= \begin{cases} l(0, v_i, \pi, \theta - \theta_i(t)) & \text{if } \sin(\theta - \theta_i(t)) < 0 \\ l(0, v_i, \frac{\pi}{4}, \theta - \theta_i(t)) & \text{if } \sin(\theta - \theta_i(t)) \geq 0 \end{cases} \\ \varphi(\rho) &= \begin{cases} \frac{1 - \cos(\frac{\pi\rho}{l_b})}{2} & \text{if } \rho < l_b \\ 1 & \text{if } \rho \geq l_b \end{cases} \end{aligned}$$

where $v_i = (-1)^i 5$. In this way each blade gives a maximum vertical speed that is equal to 5, in particular the blades at θ_0 and θ_2 give upward vertical speed while those at θ_1 and θ_3 give downward vertical speed.

4. The finite element procedure

This section is devoted to the solution of the instationary Navier-Stokes equations and the continuity equation. The general approach is the application of the Galerkin's method in the space variable ([3]).

We multiply the equations (1) and (2) by arbitrary test functions, integrate over the domain Ω and substitute boundary conditions after the use of Green Theorem. If we choose the basis functions of the approximation as test functions we end up with the Galerkin's equations.

We subdivide Ω (using [4]) into a finite number of tetrahedra satisfying the following properties:

1. if T_1 and T_2 are two tetrahedra, then either $T_1 = T_2$ or $T_1 \cap T_2 = \emptyset$ or they have a common face or a common edge or a common vertex;
2. the union of the tetrahedra is exactly Ω .

We choose a subdivision such that we have a finer refinement around C , as near C there is a large change of velocities.

The vertices of tetrahedra and the middle points of their edges are the nodes. We denote with $H = \{h_1, \dots, h_{N_H}\}$ the set of interior nodes, with $B = \{b_1, \dots, b_{N_B}\}$ the set of boundary nodes, with $K = \{k_1, \dots, k_{N_K}\}$ the set of vertices, so the set of nodes is $J = \{h_1, \dots, h_{N_H}, b_1, \dots, b_{N_B}\}$.

Let φ_j be the unique quadratic function on each tetrahedron such that $\varphi_j(j_1) = \delta_{j,j_1}$, $\forall j, j_1 \in J$ and let ϕ_k be the unique linear function on each tetrahedron such that $\phi_k(k_1) = \delta_{k,k_1}$, $\forall k, k_1 \in K$ (see [5]), where:

$$\delta_{j,j_1} = \begin{cases} 1 & \text{if } j = j_1 \\ 0 & \text{if } j \neq j_1. \end{cases}$$

We interpolate the dependent variables u_i by functions φ_j and the dependent variable p by functions ϕ_k .

This choice follows from the fact that the pressure must be approximated by interpolation polynomials that are at least one degree less than the polynomials for the velocity (see [6]), so we use a quadratic velocity approximation and a linear pressure approximation given by:

$$\begin{aligned} u_i(\mathbf{x}, t) &= u_{i0}(\mathbf{x}, t) + \sum_{h \in H} u_i^h(t) \varphi_h(\mathbf{x}), \\ u_{i0}(\mathbf{x}, t) &= \sum_{b \in B} u_i^b(t) \varphi_b(\mathbf{x}), \\ p(\mathbf{x}, t) &= \sum_{k \in K} p^k(t) \phi_k(\mathbf{x}), \end{aligned}$$

where $(u_1^j(t), u_2^j(t), u_3^j(t))$ is the speed at time t in the node j , $p^k(t)$ is the pressure at time t in the vertex k .

We note that φ_j and ϕ_k are continuously differentiable in each element and continuous in the whole domain Ω .

As test functions we choose φ_h , $h \in H$, and ϕ_k , $k \in K$, in this way $\varphi_h = 0$ on Γ .

The resulting integral equations are:

$$\begin{aligned} \int_{\Omega} \left(\frac{\partial \mathbf{u}}{\partial t} \varphi_h - \frac{1}{Re} \Delta \mathbf{u} \varphi_h + (\mathbf{u} \cdot \nabla) \mathbf{u} \varphi_h + \nabla p \varphi_h - \mathbf{f} \varphi_h \right) d\Omega &= 0, \\ \int_{\Omega} \operatorname{div} \mathbf{u} \phi_k d\Omega &= 0. \end{aligned}$$

We set $\forall i = 1, 2, 3$, $\forall h \in H$, $\forall j \in J$, $\forall b \in B$

$$\begin{aligned} \mathbf{u}_i(t) &= (u_i^{h_1}, \dots, u_i^{h_{N_H}}, u_i^{b_1}, \dots, u_i^{b_{N_B}})^T(t), \\ \mathbf{u}_i^H(t) &= (u_i^{h_1}, \dots, u_i^{h_{N_H}})^T(t), \\ \mathbf{u}_i^B(t) &= (u_i^{b_1}, \dots, u_i^{b_{N_B}})^T(t), \\ \mathbf{p}(t) &= (p^{k_1}, \dots, p^{k_{N_K}})^T(t), \\ \mathbf{f}_i(t) &= (f_i^{h_1}, \dots, f_i^{h_{N_H}})^T(t), \\ M_{h,j} &= \int_{\Omega} \varphi_h \cdot \varphi_j d\Omega, \quad M = (M^H, M^B), \\ S_{h,j} &= \frac{1}{Re} \int_{\Omega} \nabla \varphi_h \cdot \nabla \varphi_j d\Omega, \quad S = (S^H, S^B), \end{aligned}$$

$$\begin{aligned} N_{h,j}(\mathbf{u}(t)) &= \int_{\Omega} \varphi_h(\mathbf{u}(\mathbf{x},t) \cdot \nabla \varphi_j) d\Omega, \quad N = (N^H, N^B), \\ (L_i)_{k,j} &= - \int_{\Omega} \frac{\partial \varphi_j}{\partial x^i} \phi_k d\Omega, \quad L_i = (L_i^H, L_i^B), \\ f_i^h &= - \int_{\Omega} f_i \varphi_h d\Omega, \\ u_i^b(t) &= g_i(\mathbf{x}^b, t), \end{aligned}$$

where $\mathbf{x}^b = (x_1^b, x_2^b, x_3^b)$ are the coordinates of boundary node $b \in B$.

If N_T is the number of subdivision of $[0, T]$, $\Delta t = \frac{T}{N_T}$, $t_n = n\Delta t$ for $0 \leq n \leq N_T$, we use implicit Euler scheme to solve $\frac{d\mathbf{u}}{dt}$ and Picard iteration to solve $N(\mathbf{u}(t))\mathbf{u}_i(t)$.

So in our notation, we have to solve the linear system:

$$\begin{cases} \left(\frac{M^H}{\Delta t} + S^H + N^H(\mathbf{u}(t_{n-1})) \right) \mathbf{u}_i^H(t_n) + (L_i^H)^T \mathbf{p}(t_n) = \\ - \left(\frac{M^B}{\Delta t} + S^B + N^B(\mathbf{u}(t_{n-1})) \right) \mathbf{u}_i^B(t_n) + \frac{M}{\Delta t} \mathbf{u}_i(t_{n-1}) + \mathbf{f}_i(t_n) \\ L_1^H \mathbf{u}_1^H(t_n) + L_2^H \mathbf{u}_2^H(t_n) + L_3^H \mathbf{u}_3^H(t_n) = -L_1^B \mathbf{u}_1^B(t_n) - L_2^B \mathbf{u}_2^B(t_n) - L_3^B \mathbf{u}_3^B(t_n) \end{cases}$$

$\forall i = 1, 2, 3, \forall 1 \leq n \leq N_T$.

5. Qualitative and quantitative measures of mixing phenomena

Now, having computed the flow field $\mathbf{u}(\mathbf{x}, t)$, we want to analyze the mixing process. An accurate determination of the mixing phenomena can be obtained by calculating the trajectories of fluid particles in the flow field of the mixer. Such an approach, which can be applied to a part of the fluid, has been adopted for the present study. To obtain an accurate global evaluation of the mixing, it is necessary to study the trajectories of a large number of particles, leading to the use of a massively parallel computer system.

Some care must be taken at the integrating of the equation for the streamlines in order to retain a sufficient degree of accuracy. For the result presented in this paper, we used a two-step Adams-Bashforth scheme.

If $\xi^p(t)$ is the position of a point p at time t , and ξ_0^p is its initial position, we have:

$$\begin{cases} \frac{d\xi^p}{dt} = \mathbf{v}(\xi^p, t), \quad \forall t \in [0, T] \\ \xi^p(0) = \xi_0^p \end{cases}$$

where $\mathbf{v}(\xi^p, t)$ is the speed of the particle p at time t and it is given by:

$$\mathbf{v}(\mathbf{x}, t) = \begin{cases} \mathbf{u}(\mathbf{x}, t), & \forall t \in [0, T], \forall \mathbf{x} \in \Omega \\ \mathbf{g}(\mathbf{x}, t), & \forall t \in [0, T], \forall \mathbf{x} \in C. \end{cases}$$

We subdivide $[0, T]$ in N_T subintervals and we have a time step $\Delta t = \frac{T}{N_T}$, $t_n = n\Delta t$ for $0 \leq n \leq N_T$. Using second order Adams-Bashforth method, we have $\forall 1 \leq n \leq N_T$

$$\xi^p(t_{n+1}) = \xi^p(t_n) + \frac{\Delta t}{2} (3\mathbf{v}(\xi^p(t_n), t_n) - \mathbf{v}(\xi^p(t_{n-1}), t_{n-1})).$$

Note that $\mathbf{v}(\mathbf{x}, 0) = \mathbf{0} \forall \mathbf{x}$, since initially the fluid and the impeller are steady.

Solving these equations we find the position of particle p at each time step, so we can supervise the displacement of the particles, under the action of the turbine.

To analyze the mixing phenomena, in the first simulation, particle trajectories corresponding to only a part of the fluid have been calculated.

We consider the following grid of $\Omega \cup C$, with step $\sigma = 0.03$:

$$G = \{\mathbf{x} \in \Omega \cup C : x_1 = -r_m + i_1\sigma, x_2 = -r_m + i_2\sigma, x_3 = i_3\sigma, i_1, i_2, i_3 \in \mathbb{N}\},$$

where $r_m = \max\{r_i, r_s\}$ and we compute the trajectories of a set of particles P , setting in $S \cap G$ at $t = \Delta t$, where $S = \{\mathbf{x} \in \Omega \cup C : \frac{z_m + z_M}{2} - 0.15 \leq x_3 \leq \frac{z_m + z_M}{2} + 0.15, 0.0 \leq x_1, x_2 \leq r_m\}$.

We obtain a visualization of the mixing phenomena drawing (using [7]) the isosurface of the function $\delta : G \rightarrow \mathbb{R}$ defined in the following way:

$$\delta_p(g) = \begin{cases} e^{\frac{d_{g,p}}{d_{g,p} - \epsilon}} & \text{if } d_{g,p} < \epsilon \\ 0 & \text{if } d_{g,p} \geq \epsilon \end{cases}$$

$$\delta(g) = \sum_{p \in P} \delta_p(g),$$

where $d_{g,p}$ is the distance between p and g , and $\epsilon = 2\sigma$.

For other evaluations of the mixing phenomena we follow particles of P_s for $s = 1, \dots, 4$, that at $t = \Delta t$ are respectively located in $B_s = \{(id_1 \cos \frac{k\pi}{8}, id_1 \sin \frac{k\pi}{8}, jd_2 + \frac{d_2}{2}) : 0 \leq k \leq 7, 3 + 6k \leq i \leq 50, 3 + 6(s-1) \leq j \leq 3 + 6s - 1\}$, where $d_1 = \frac{\max\{r_s, r_i\}}{75}$ and $d_2 = \frac{z_s}{150}$.

In order to have some quantitative measures of flow mixing, first we subdivide $\Omega \cup C$ in 1100 bins with height $3d_2$ and base 0.13×0.13 , and consider the following dispersion indices (see [8]):

$$\sigma'(t) = \frac{\text{number of bins occupied by particles of } \cup_{s=1}^4 P_s \text{ at time } t}{1100},$$

$$\sigma''(t) = \frac{\text{number of bins occupied by particles of } \cup_{s=2}^3 P_s \text{ at time } t}{1100}.$$

Then we subdivide $\Omega \cup C$ into 72 layers:

$$L_k = \left\{ \mathbf{x} \in \Omega \cup C : \left(2k + \frac{3}{2}\right)d_2 \leq x_3 < \left(2k + \frac{7}{2}\right)d_2 \right\} \quad k = 1, \dots, 72$$

and consider the following diffusion indices:

$$\rho_s(t, k) = \frac{\text{number of particles of } P_s \text{ in } L_k \text{ at time } t}{10 \text{ Volume}(L_k)}.$$

6. Results and conclusions

For our simulation we get $T = 7$ and $N_T = 700$ and we consider three cases.

In the first case the geometry Ω_1 is given by $r_i = 0.4$, $r_s = 0.6$, $z_s = 1.5$, $l_b = r_C = 0.25$, $z_m = 0.4$, $z_M = 0.5$, the function that simulates the blade turbine gives only a radial impulse to the fluid, Ω_1 is divided into 2114 tetrahedra and the resulting mesh gives $N_H = 2471$, $N_B = 712$, $N_K = 439$, $Re = 100$.

In the second case the geometry Ω_2 is given by $r_i = 0.45$, $r_s = 0.65$, $z_s = 1.6$, $l_b = r_C = 0.275$, $z_m = 0.24$, $z_M = 0.34$, the function that simulates the blade turbine gives also a vertical impulse to the fluid, Ω_2 is divided into 19712 tetrahedra and the resulting mesh gives $N_H = 24820$, $N_B = 3028$, $N_K = 3691$, $Re = 250$.

In the third case the geometry Ω_3 is given by $r_i = 0.65$, $r_s = 0.45$, $z_s = 1.6$, $l_b = r_C = 0.275$, $z_m = 0.24$, $z_M = 0.34$, the function that simulates the blade turbine gives also a

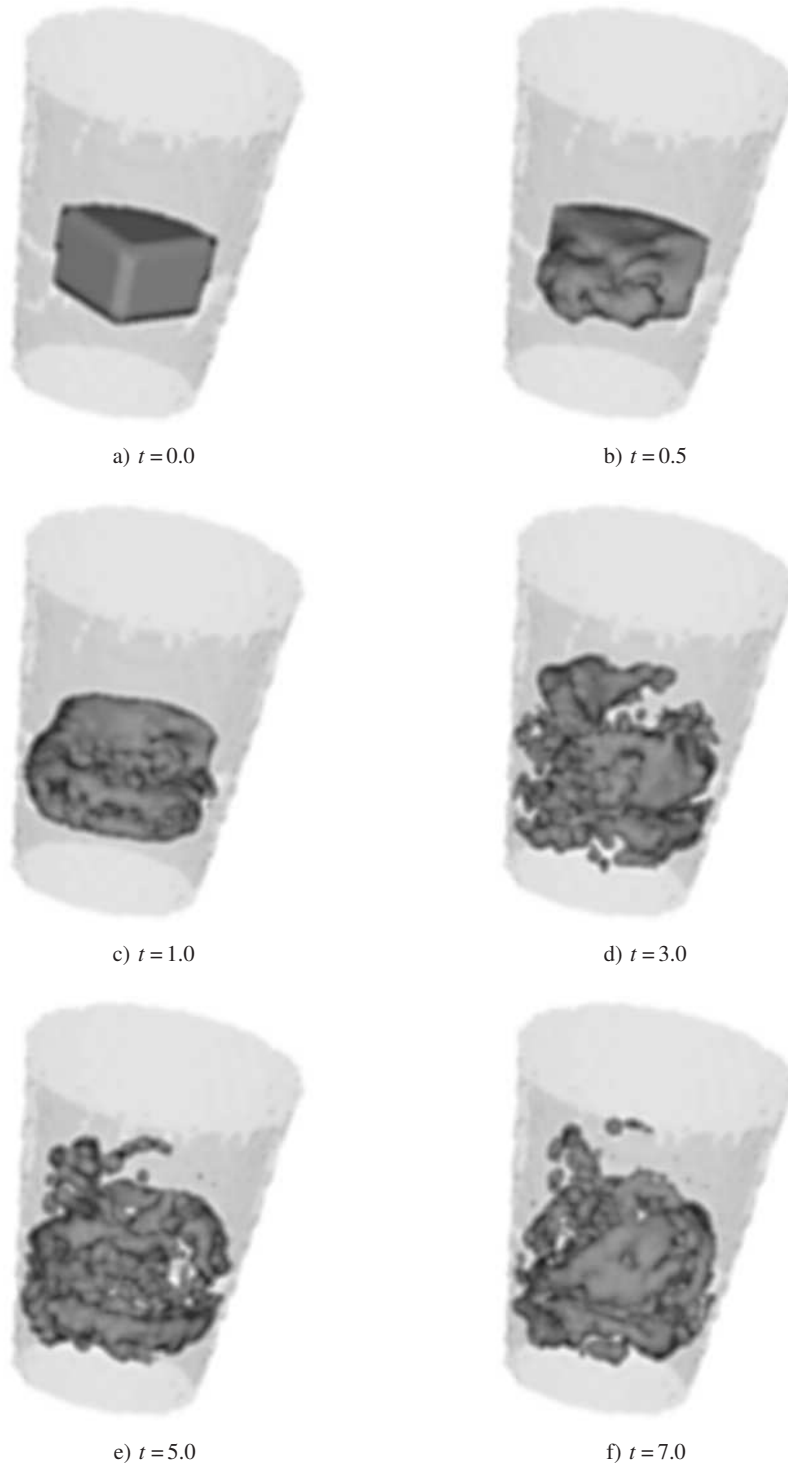


Figure 1. Isosurface $\delta=0.61$ in Ω_1 , the considered particles of P are 2149

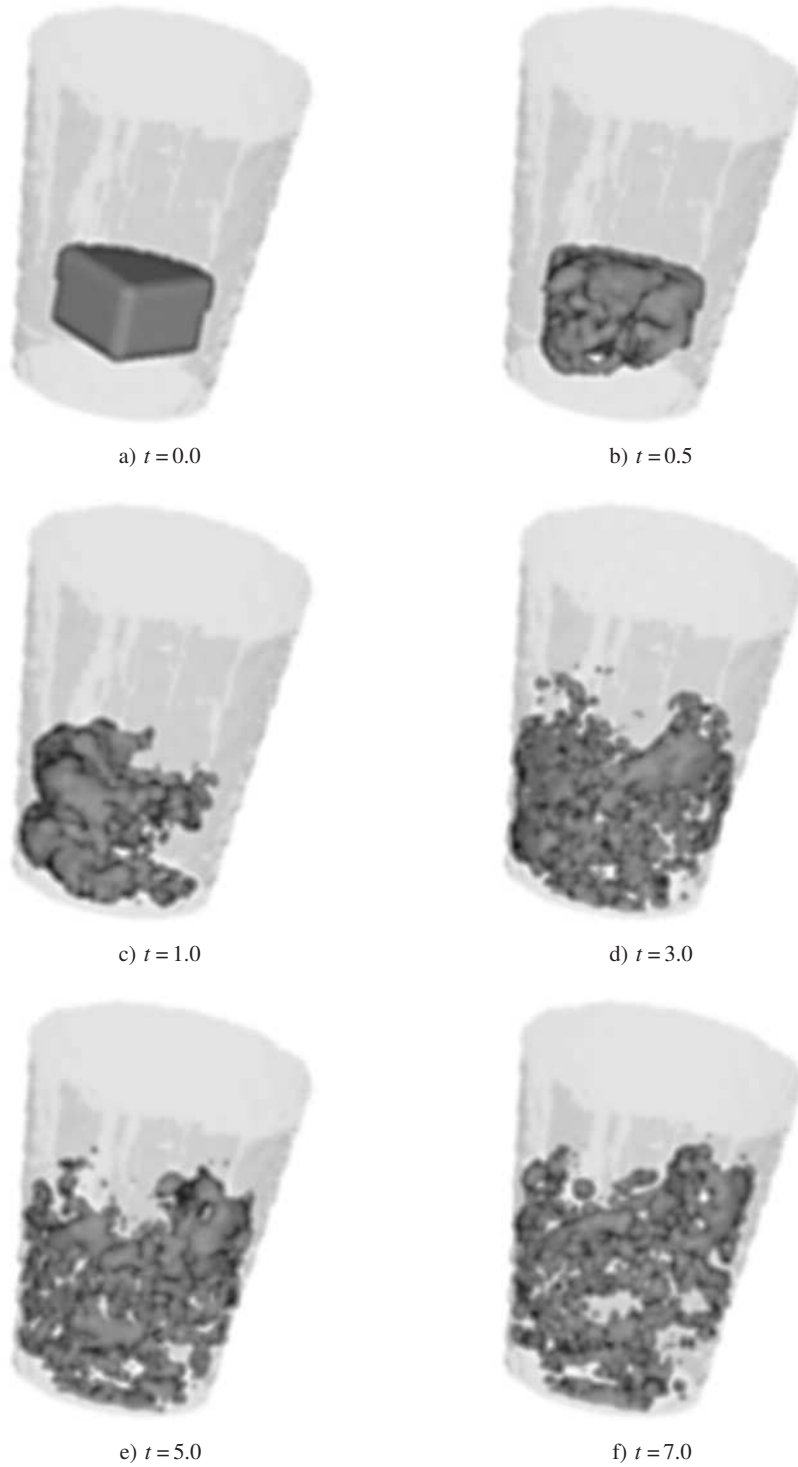


Figure 2. Isosurface $\delta=0.61$ in Ω_2 , the considered particles of P are 2086

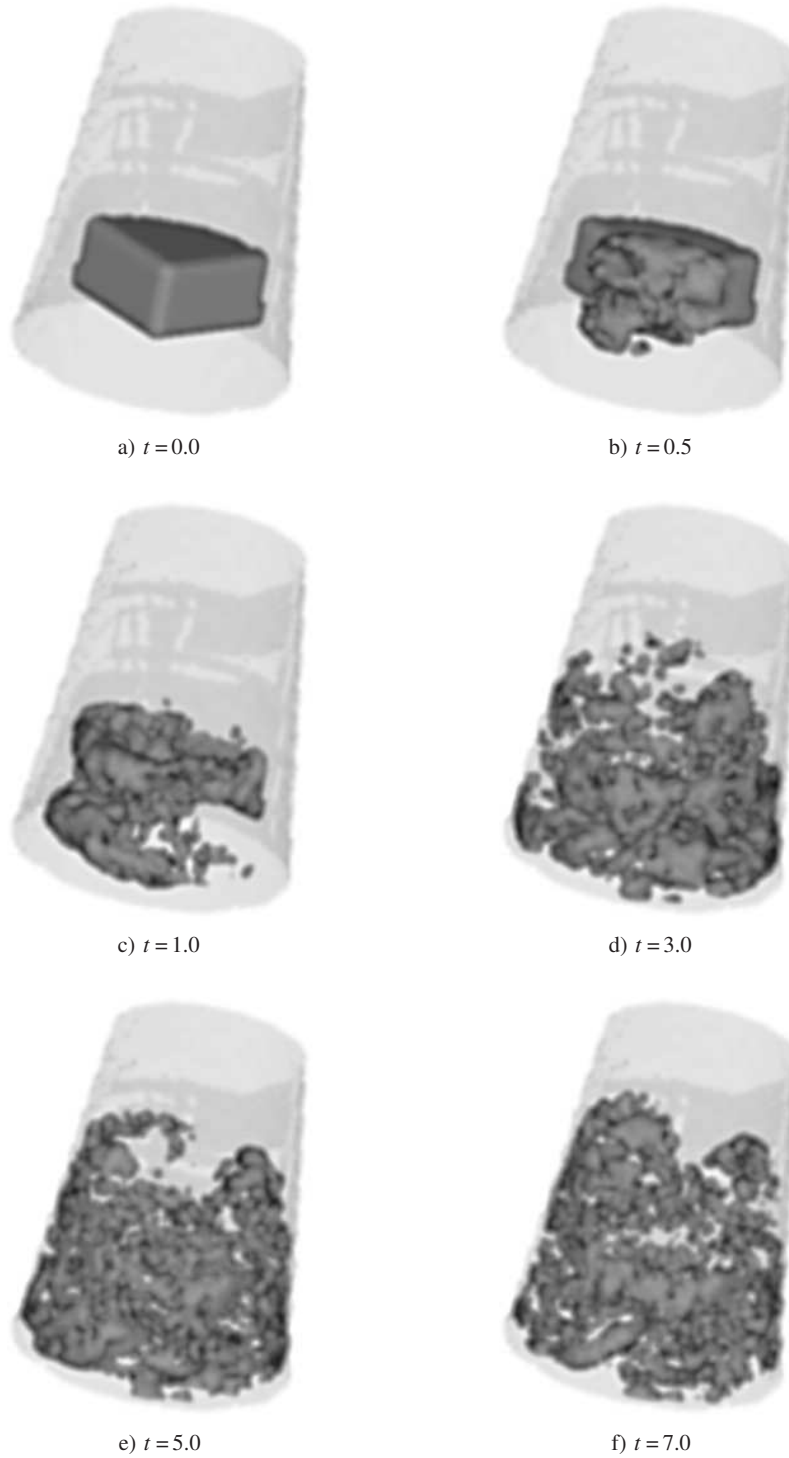


Figure 3. Isosurface $\delta = 0.61$ in Ω_3 , the considered particles of P are 3285



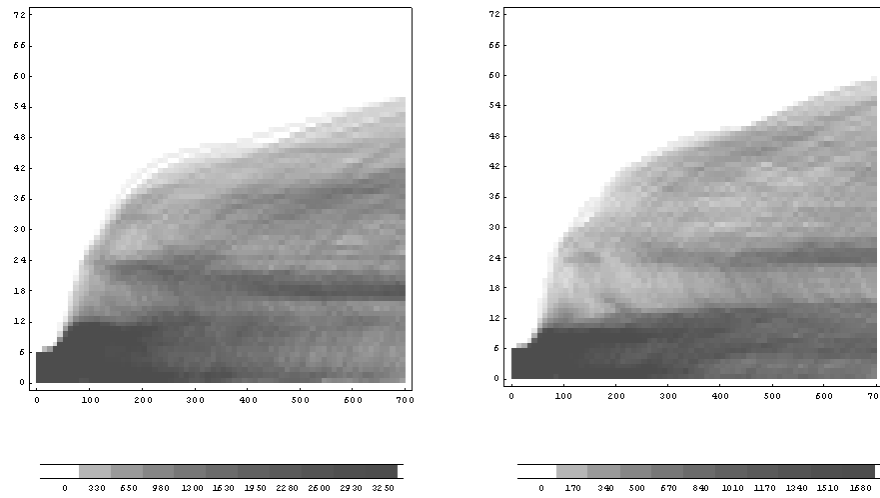


Figure 4. $\rho_1(\frac{n}{100}, k)$, $k = 1, \dots, 72$, $0 \leq n \leq 700$, Ω_2 on the left and Ω_3 on the right

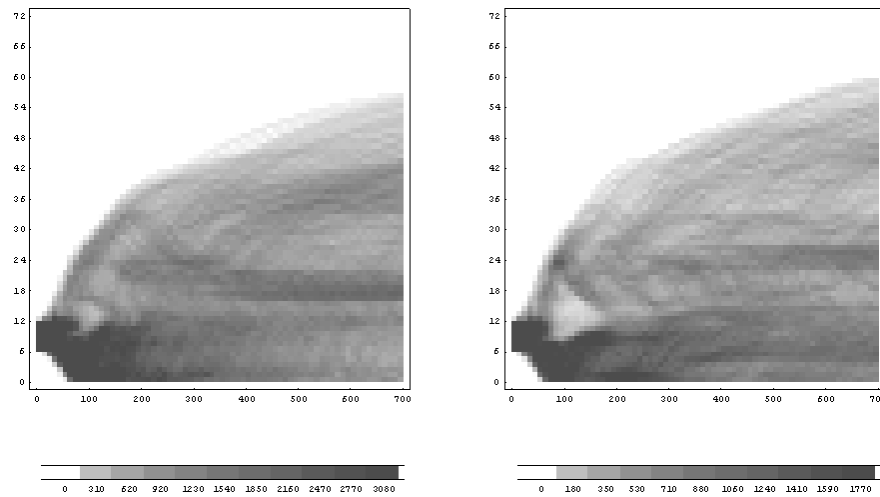


Figure 5. $\rho_2(\frac{n}{100}, k)$, $k = 1, \dots, 72$, $0 \leq n \leq 700$, Ω_2 on the left and Ω_3 on the right

vertical impulse to the fluid, Ω_3 is divided into 19864 tetrahedra and the resulting mesh gives $N_H = 25008$, $N_B = 3044$, $N_K = 3715$, $Re = 250$.

We note that since we consider only a discrete set of non-interacting particles we have value of δ greater than the initial maximum, moreover the plots of isosurface (Figures 1–3), at different time, illustrate that the redistribution of the particles varies with the Reynolds number of the flow, with the geometry of the mixer and with the type of blades push.

In particular in Ω_1 (Figure 1) the mixing is poor since there is no vertical contribute from the turbine and the Reynolds number is lower than in the other cases.

From the diffusion indices, Figures 4–7, we can see that in Ω_3 the particles reach higher levels than in Ω_2 , independentment from their initial position, so there is a better diffusion in Ω_3 .

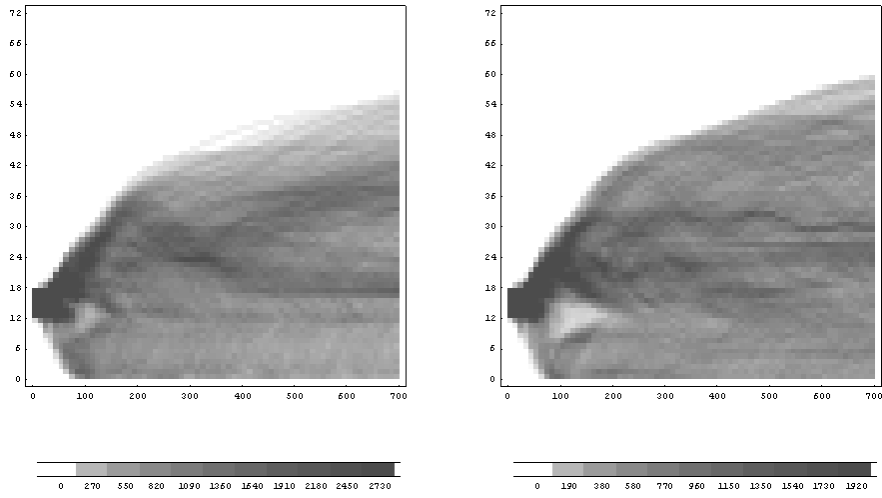


Figure 6. $\rho_3(\frac{n}{100}, k)$, $k = 1, \dots, 72$, $0 \leq n \leq 700$, Ω_2 on the left and Ω_3 on the right

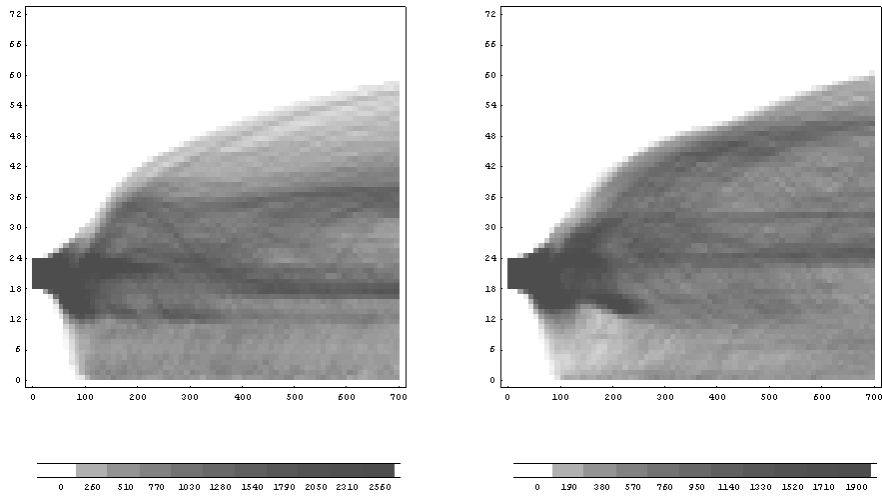


Figure 7. $\rho_4(\frac{n}{100}, k)$, $k = 1, \dots, 72$, $0 \leq n \leq 700$, Ω_2 on the left and Ω_3 on the right

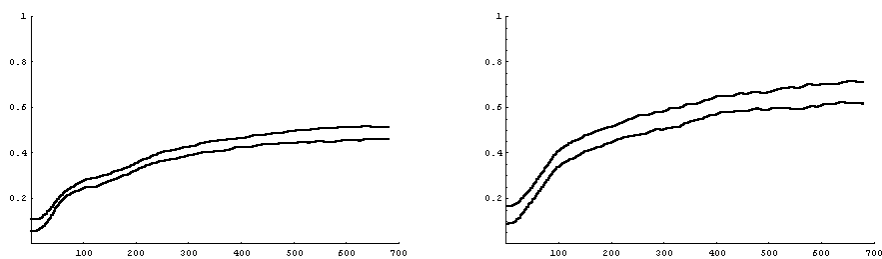


Figure 8. The upper curve shows $\sigma'(\frac{n}{100})$, the lower curve shows $\sigma''(\frac{n}{100})$, Ω_2 on the left and Ω_3 on the right

From the dispersion indices, Figure 8, starting from particles of $\cup_{s=1}^4 P_s$ or from particles of $\cup_{s=2}^3 P_s$, we see that the number of bins occupied is greater in Ω_3 than in Ω_2 .

If we consider Figures 2 and 3 we can say that the mixing is better in Ω_3 than in Ω_2 , the only difference between them being the geometry. This result might be an artefact because the number of considered particles, at time $t=0$, is greater in Ω_3 than in Ω_2 . For this reason we have introduced the indices of diffusion and dispersion. From the comparison of the dispersion indices, Figure 8, and of the diffusion indices, Figures 4–7, for the same fluid and the same rotor turbine, we can affirm that the mixing in Ω_3 is better than in Ω_2 .

Nevertheless we observe that for $t=7$ the layers near the top do not show trace of the perturbation given by the turbine, so the results might be different for large values of t .

References

- [1] Anderson J D Jr 1995 *Computational Fluid Dynamics, the basics with applications* McGraw-Hill International Editions
- [2] Ladyzhenskaya O A 1969 *The Mathematical Theory of Viscous Incompressible Flow* Gordon and Breach
- [3] Quarteroni A, Valli A 1994 *Numerical Approximation of Partial Differential Equations* Springer
- [4] Schöleb J 2000 *Neigen-4.0 SFB Numerical and Symbolic Scientific Computing* Johannes Kepler Universität Linz, Austria
- [5] Cuvelier C, Segal A, van Steenhoven A A 1986 *Finite Element Methods and Navier-Stokes Equations* D. Reidel Publishing Company
- [6] Finlayson B A 1992 *Numerical Methods for Problems with Moving Fronts* Ravenna Park Publishing Inc., Seattle, Washington
- [7] Hibbard B, Paul B, Battaiola A *Vis5d Version 3.0*
- [8] Liu M, Andreasen C D, LaRoche R D, Choudhary S *Visualization and Quantification of Laminar Flow Mixing in a Stirred Tank Reactor* document available from: <http://www.cpcfd.org/laroche>.

